



Sub-micron particle number size distributions characteristics at an urban location, Kanpur, in the Indo-Gangetic Plain



V.P. Kanawade*, S.N. Tripathi, Deepika Bhattu, P.M. Shamjad

Department of Civil Engineering & Center for Environmental Science and Engineering, Indian Institute of Technology Kanpur, Kanpur 208016, India

ARTICLE INFO

Article history:

Received 7 February 2014

Received in revised form 20 April 2014

Accepted 14 May 2014

Available online 22 May 2014

Keywords:

Particle number concentration

Aitken mode

Seasonal variation

Black carbon

ABSTRACT

We present long-term measurements of sub-micron particle number size distributions (PNSDs) conducted at an urban location, Kanpur, in India, from September 2007 to July 2011. The mean Aitken mode (N_{AIT}), accumulation mode (N_{ACCU}), the total particle (N_{TOT}), and black carbon (BC) mass concentrations were $12.4 \times 10^3 \text{ cm}^{-3}$, $18.9 \times 10^3 \text{ cm}^{-3}$, $31.9 \times 10^3 \text{ cm}^{-3}$, and $7.96 \mu\text{g m}^{-3}$, respectively, within the observed range at other urban locations worldwide, but much higher than those reported at urban sites in the developed nations. The total particle volume concentration appears to be dominated mainly by the accumulation mode particles, except during the monsoon months, perhaps due to efficient wet deposition of accumulation mode particles by precipitation. At Kanpur, the diurnal variation of particle number concentrations was very distinct, with highest during morning and late evening hours, and lowest during the afternoon hours. This behavior could be attributed to the large primary emissions of aerosol particles and temporal evolution of the planetary boundary layer. A distinct seasonal variation in the total particle number and BC mass concentrations was observed, with the maximum in winter and minimum during the rainy season, however, the Aitken mode particles did not show a clear seasonal fluctuation. The ratio of Aitken to accumulation mode particles, N_{AIT}/N_{ACCU} , was varied from 0.1 to 14.2, with maximum during April to September months, probably suggesting the importance of new particle formation processes and subsequent particle growth. This finding suggests that dedicated long-term measurements of PNSDs (from a few nanometer to one micron) are required to systematically characterize new particle formation over the Indian subcontinent that has been largely unstudied so far. Contrarily, the low N_{AIT}/N_{ACCU} during post-monsoon and winter indicated the dominance of biomass/biofuel burning aerosol emissions at this site.

© 2014 Elsevier B.V. All rights reserved.

1. Introduction

Atmospheric aerosol particles are ubiquitous, which impact not only global climate but also human health, air quality and visibility. Nowadays, the effects of particles on human health are of serious concern in urban areas, particularly for nations with very fast changing economies, such as India and China. As per the National Ambient Air Quality Monitoring Program

(NAAQMP) in India, particulate matter less than $10 \mu\text{m}$ (PM_{10}) has the highest exceedance rate, followed by nitrogen dioxide (NO_2) and sulfur dioxide (SO_2). The $\text{PM}_{2.5}$, which is not widely monitored in India, is expected to be even worse (CPCB, 2012). To quote few facts from recent studies, Ramanathan et al. (2008) estimated that an increase in anthropogenic $\text{PM}_{2.5}$ concentration of $2.5 \mu\text{g m}^{-3}$ from its current value would result in 337,000 excess deaths per year, owing to outdoor exposure to air pollution in India, and exposure to indoor pollution attributable to solid fuel use is estimated to cause an additional 407,100 deaths in India. Aerosol particles also reduce incoming solar radiation to the surface in India by

* Corresponding author. Tel.: +91 512 2596224.

E-mail address: vijaykanawade03@yahoo.co.in (V.P. Kanawade).

about 15 W m^{-2} or more, compared with pre-industrial values, causing solar dimming (Padma Kumari et al., 2007; Ramanathan et al., 2008) as well as reduced visibility (Singh and Dey, 2012; Wang et al., 2009). A statistically significant increasing trend in aerosol loading, about $2.3\% \text{ year}^{-1}$ of its value in 1985 and more rapidly $\sim 4\% \text{ year}^{-1}$ during the last decade, over India was also observed (Moorthy et al., 2013). Moreover, black carbon (BC) aerosols, with the second or third largest global warming potential have not only attracted atmospheric and climatic scientists' attention but also attracted policy makers' due to its adverse human health effects. Thus, the observation of sub-micron particles over a wide size range (from a few nanometer to one micron), BC and chemical composition over an extended period of time is crucial to evaluate their effects on human health, the environment, air quality and the climate over Indian subcontinent, where long-term datasets are scarce, or available as a whole for only a few locations in an air quality networks.

Until now, numerous researchers have carried out continuous measurements of sub-micron particle number size distributions (PNSDs) at a variety of locations to examine their diurnal patterns and seasonal variations. Table 1 summarizes such long-term measurements of sub-micron PNSDs from selected urban areas across the globe. In these studies, the temporal evolution of particle number concentrations showed pronounced seasonal variation with lower concentrations in summer and higher concentrations during winter, whereas the diurnal patterns were mostly found to be strongly influenced by vehicular emissions. A pronounced increase in particle number concentrations, particularly the Aitken mode particles, was also observed during traffic hours (Stanier et al., 2004). Thus, the vehicular emissions have been considered as one of the major sources of aerosol loading in urban areas. Besides, the formation of new particle (i.e. nucleation) is also a further, and important, source of particles in the atmosphere (Kulmala, 2003; Shi and Harrison, 1999; Zhang, 2010). Several studies have also examined new particle formation (NPF) characteristics in diverse environments (Kulmala et al., 2004), including

middle-upper troposphere (Kanawade and Tripathi, 2006), Finland boreal forest site (Makela et al., 1997), rural site (Weber et al., 1997), semi-rural site (Kanawade et al., 2012) as well as urban areas (Kanawade et al., personal communication; McMurry et al., 2005; Mönkkönen et al., 2005; Stanier et al., 2004; Young et al., 2013). These newly formed particles may further account for 3–70% of the global CCN production in the troposphere (Matsui et al., 2013; Pierce and Adams, 2009).

In India, there are several long-term studies on aerosol physical and optical properties based on satellite datasets (Dey and Di Girolamo, 2011; Kaskaoutis et al., 2013; Ramachandran et al., 2013), Aerosol Robotic Network (AERONET) measurement stations (Dey and Tripathi, 2008; Eck et al., 2010; Kaskaoutis et al., 2012; Singh et al., 2004), and Aerosol Radiative Forcing over India NETwork (ARFINET) (Moorthy et al., 2013). However, to the best of our knowledge, there are currently no reports published on long-term measurements of sub-micron PNSDs in urban areas of India, except two studies which examined seasonal characteristics of PNSDs at the semi-urban site, Gual Pahari (Hyvarinen et al., 2010), and the Himalayan background site, Mukteshwar (Komppula et al., 2009).

Here, we analyze four-year measurements of sub-micron PNSD to examine diurnal patterns of size-segregated particle number concentrations and seasonal variations of particle size distributions at an urban location, Kanpur, in the Indo-Gangetic Plain (IGP) of India. We measured PNSDs using a scanning mobility particle sizer (SMPS) in the size range of 13.8–685 nm at Kanpur during September 2007–July 2011. Simultaneously, BC measurements were also made using the seven channel Aethalometer. Previously, we have analyzed PNSDs (Baxla et al., 2009) and BC mass concentrations (Ram et al., 2010) from ~ 1 year of measurements at this site, but the present study focuses on statistical analysis of long-term measurements of PNSD, in particular for an improved understanding of atmospheric aerosol processes, and BC, due to its importance for climatic and human health studies over this region (Ramanathan et al., 2008).

Table 1

Comparison of total particle number concentrations at Kanpur with those reported from other urban locations worldwide based on long-term observations.

Location	Lat. [deg.]	Long. [deg.]	Site type	Period [month/year]	Size range [nm]	Particle conc. [$N_{\text{TOT}}, 10^3 \text{ cm}^{-3}$]	Reference
Kanpur, India	26.46	80.32	Urban	12/2006–11/2011	14–685	31.9 ± 29.7	This study
Beijing, China	39.54	116.23	Urban	03/2004–03/2006	3–1000	32.7	(Wu et al., 2008)
Pittsburgh, USA	40.44	–80.00	Urban	07/2001–06/2002	3–500	22.0	(Stanier et al., 2004)
Atlanta, USA	33.76	–84.39	Urban	08/1998–08/1999	10–100	21.4	(Woo et al., 2001)
Rochester, NY, USA	43.16	–77.60	Urban	01/2002–12/2009	10–500	7.6	(Wang et al., 2011a)
Birmingham, UK	52.48	–1.89	Urban	10/2002–03/2004	7–3000	18.8	(Puustinen et al., 2007)
London, UK	51.52	0.13	Urban	04/2004–04/2005	10–415	11.4	(Rodríguez et al., 2007)
Milan, Italy	45.48	9.17	Urban	11/2003–12/2004	10–800	25.8	(Rodríguez et al., 2007)
Barcelona, Spain	41.38	2.12	Urban	11/2003–12/2004	10–800	16.8	(Rodríguez et al., 2007)
Leipzig, Germany	51.33	12.38	Urban	02/1997–02/2001	3–800	21.0	(Wehner and Wiedensohler, 2003)
Bern, Switzerland	46.95	7.44	Urban	01/2009–12/2009	7–1000	28.0	(Reche et al., 2011)
Huelva, Spain	37.25	6.95	Urban	01/2009–12/2009	3–10,000	17.9	(Reche et al., 2011)
Helsinki, Finland	60.16	24.95	Urban	01/1998–12/2000	8–400	17.2	(Hussein et al., 2004)
Budapest, Hungary	47.47	19.06	Urban	11/2008–11/2009	6–1000	11.8	(Salma et al., 2011)
Amsterdam, Netherlands	52.37	4.89	Urban	10/2002–03/2004	7–3000	18.1	(Puustinen et al., 2007)
Athens, Greece	37.96	23.71	Urban	10/2002–03/2004	7–3000	20.3	(Puustinen et al., 2007)
Brisbane, Australia	–27.5	153.0	Urban	07/1995–11/2000	15–630	5–17	(Mejía et al., 2007)
Gual Pahari, India	28.43	77.15	Semi-urban	11/2007–01/2010	4–10,000	21.8	(Hyvarinen et al., 2010)
Mukteshwar, India	29.43	79.62	Background	11/2005–11/2008	10–800	2.7	(Komppula et al., 2009)

2. Experimental setup and methods

2.1. Sampling site

The measurements were carried out from the second floor of the Western Laboratory building inside the Indian Institute of Technology Kanpur (IITK) campus (26.46°N, 80.32°E, 125 m amsl). The IITK campus is located about 16 km away from the Kanpur city center to the northwest. The Grand-Trunk (G-T) road, with a moderately intense traffic, is located about 600 m to the east of the IITK sampling site (Fig. 1). The G-T road (National Highway 91) connects Kanpur to the metropolitan city, New Delhi. Heavy-duty trucks are allowed to take the G-T road only during nighttime between 9:00 PM and 7:00 AM, but there are local public transport buses and other traffic vehicles (2-, 3-, and 4-wheelers) running all day. As per 2011 census report, Kanpur has a population of ~4.5 million inhabitants, with about 1452 people km⁻². It is located in one of the biggest industrial hubs in the IGP in Northern India, and a large number of coal-burning thermal power plants are clustered along this region. The nearest major coal-burning thermal power plant is located ~3 km aerial distance from the IITK site to the southeast. Besides, a few brick kilns are also located in the surroundings of the IITK site. The IGP region continuously produces anthropogenic pollution from urban,

industrial, and rural combustion sources, causing large primary aerosol loading almost throughout the year. The annual mean concentration of PM₁₀ for major urban centers in the IGP region is higher than the rest of India, with about 1.5 to 4.4 times higher concentration than the National Ambient Air Quality Standard (NAAQS) value (Table S1). A recent study also found a significant increasing trend in aerosol optical depth (AOD) of 7.69% year⁻¹ over Kanpur for 2001–2010 (Kaskaoutis et al., 2012). Automobiles are thought to be the major source of air pollution followed by industrial, biomass burning, residential cooking, and agricultural land clearing (Ramanathan and Ramana, 2005; Tripathi et al., 2006). Moreover, the IITK site is also affected by desert and alluvial dust particles during the pre-monsoon season (Chinnam et al., 2006; Dey et al., 2004). The prevailing northwesterly and southeasterly winds are also conducive for transport of air pollutant from the northwest and southeast IGP region to the downwind IITK site in the central IGP, respectively (Fig. S1).

2.2. Measurement techniques and data processing

PNSDs were measured with a scanning mobility particle sizer (SMPS, TSI 3696) using a long-differential mobility analyzer (LDMA) in combination with a butanol based condensation particle counter (CPC) in which particles are

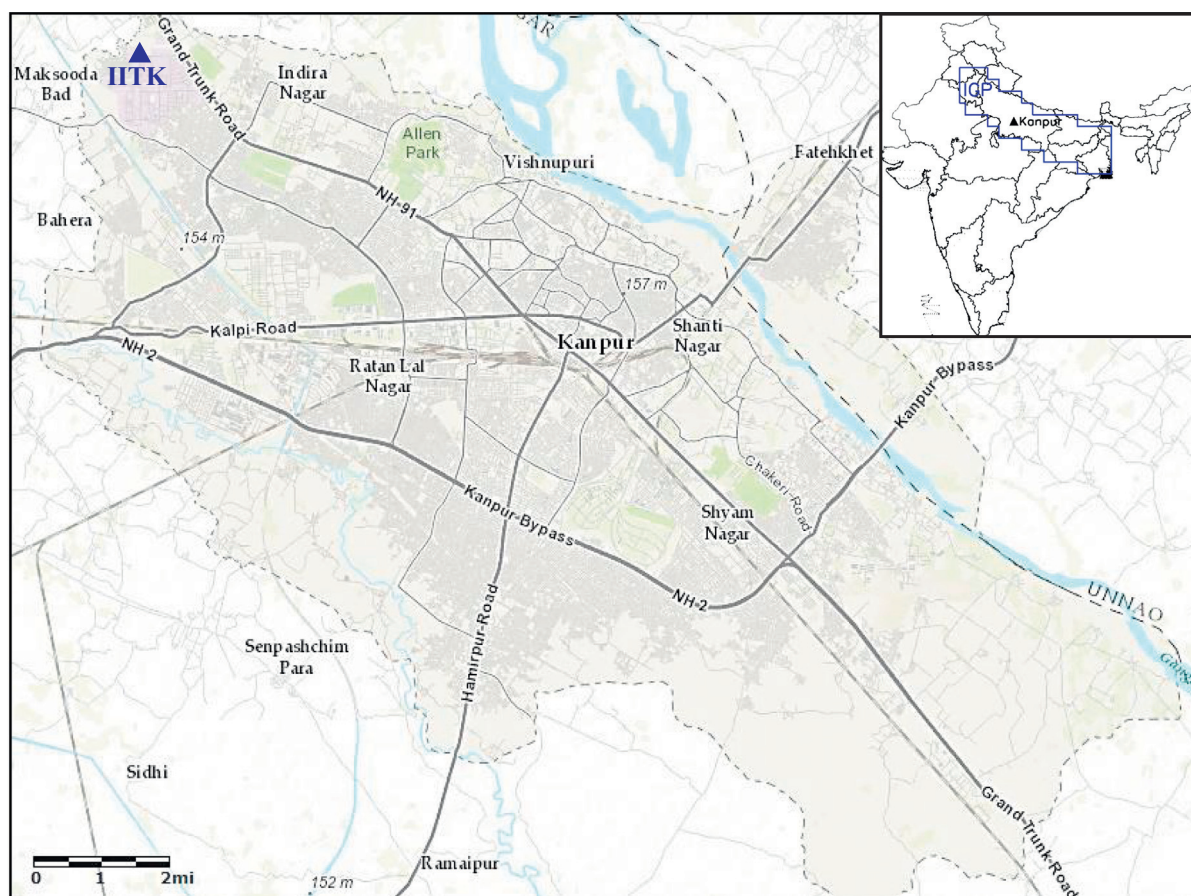


Fig. 1. Location of the sampling site, Kanpur, in the Indo-Gangetic Plain. A city-scale map was obtained from the website www.arcgis.com.

neutralized by a radioactive source (85 Kr) before being selected in the DMA. The detectable aerosol mobility diameter ranged from 13.8 to 685 nm (109 size bins) with a sheath and sample flow rates of 3.0 lpm and 0.3 lpm, respectively. Aitken, accumulation, and total particle number concentrations were derived by integrating the number concentration of particles in the size range of 20–100 nm, 100–685 nm, and 14–685 nm, respectively. These concentrations hereafter are denoted as N_{AIT} , N_{ACCU} , and N_{TOT} , respectively. The total surface area and volume concentrations were also calculated in the particle size range of 14–685 nm, hereafter denoted as SA_{TOT} and Vol_{TOT} , respectively. The particle mode diameter (i.e. local maxima of the size distribution) was also derived, hereafter denoted as $D_{\text{p,mode}}$. The BC mass concentration was measured using an Aethalometer (AE-42, Magee Scientific) at seven wavelengths (370, 470, 520, 590, 660, 880, and 950 nm), with a flow rate of 2.0 lpm. The BC data was obtained every 5 min and corrected for two effects (“multiple scattering” and “shadowing”) which change the optical properties of filter embedded particles with respect to the properties of the same particles in the airborne state. A constant value of 2.14 was used for the multiple scattering of the light beam at the filter fibers in the unloaded filter and the shadowing effect was assumed to be negligible, particularly for aged BC particles (Weingartner et al., 2003). Here, we used mass concentrations at 370 nm and 880 nm to infer the key local source (i.e. wood burning vs fossil fuel combustion) of brown carbon (BrC) aerosols at this site. The concentration at 370 nm will have mass from both the BrC and BC, while the mass at 880 nm will be pure BC. More details about the Aethalometer are described elsewhere (Tripathi et al., 2005). Meteorological parameters such as ambient air temperature, relative humidity, wind speed, and wind direction were measured simultaneously at the Indian Space Research Organization’s (ISRO) automatic weather station (AWS-ES, ISRO20) installed inside the IITK campus. Air temperature and relative humidity were measured with an accuracy of ± 0.2 °C and $\pm 3\%$, respectively. Wind speed and wind direction were measured with an accuracy of 0.5 m s^{-1} and 3° , respectively (Table S2). Air mass backward trajectories and mixed depth (MD) were calculated with the National Oceanic and Atmospheric Administration (NOAA) Air Resources Laboratory (ARL) Hybrid Single-Particle Lagrangian Integrated Trajectory (HYSPLOT) PC version model (Draxler and Rolph, 2010) and using gridded wind fields from the Global Data Assimilation System (GDAS), with a spatial resolution of $1^\circ \times 1^\circ$ and a time resolution of 1 h (Kanamitsu, 1989). Here, we split long-term dataset into four different seasons i.e. winter (December–February), pre-monsoon (March–May), monsoon (June–August) and post-monsoon (September–November) (Singh et al., 2004).

2.3. Data coverage

Here, we presented nearly four-years of semi-continuous measurements. The overall monthly coverage was adequate for determining key characteristics of the PNSDs and BC. There were some short- as well as long-time missing data periods. The main reasons for the measurement interruptions were calibrations, instrument malfunctioning, or usage by our research colleagues as a part of a short-period of time measurement campaigns (Jai Devi et al., 2011; Joshi et al.,

2012; Roy et al., 2009; Shamjad et al., 2012; Srivastava et al., 2013). Fig. 2 shows the percentage of sampling days in individual months, summed over the entire measurement period for both SMPS and Aethalometer. Despite the data gaps, we have about 50% of the available data from both instruments, which is quite reasonable to perform statistical analyses.

3. Results and discussion

3.1. General description of meteorological conditions

Meteorological conditions for Kanpur show strong seasonal variation. Fig. S2 shows the monthly statistical analysis of ambient air temperature and relative humidity. The lowest and highest ambient temperatures were observed in January and June with the mean value of 12.1 °C and 32 °C, respectively. The monthly mean minimum and maximum temperatures were 2 °C and 45.2 °C in January and June, respectively (Fig. S2a). The mean relative humidity in pre-monsoon ($\sim 48\%$) tended to be lower than the values in Monsoon ($\sim 80\%$) (Fig. S2b). Northern India experiences southwest monsoon, which is associated with the movement of the Inter-Tropical Convergence Zone (ITCZ) in June each year (Asnani, 1993). The southwest monsoon winds occur during June to September brings mixed (marine and continental) air mass influx over the Northern India when the ITCZ moves northward reaching as north as 30°N . The seasonal frequency distribution of wind direction and wind speed based on hourly averages is shown in Fig. S3. Overall, the light winds with speed less than 1 m s^{-1} are predominant throughout the year, with the mean hourly wind speed varying from 0.1 to 7.4 m s^{-1} . The northwesterly and east-southeasterly flows are mostly dominant during the winter season (33% and 27%) followed by pre-monsoon (26% and 21%), and post-monsoon (24% and 15%), respectively. In the monsoon season, the southwesterly flow is most noticeable (42%) with less prominent northwesterly (11%) and east-southeasterly (12%) flows.

3.2. Diurnal and monthly variation of particle number and BC mass concentrations

In order to examine general aerosol behavior at this site, we have performed statistical analysis of particle number (in three different size modes), total surface, total volume, and BC mass concentrations. This kind of aerosol dataset analysis is handy to understand aerosol characteristics at the regional scale as well as at different meteorological conditions when compared with other locations worldwide. Statistical parameters for Aitken mode (N_{AIT}), accumulation mode (N_{ACCU}), total particle number (N_{TOT}), total surface area (SA_{TOT}), total volume (Vol_{TOT}), BC mass concentrations, and particle mode diameter ($D_{\text{p,mode}}$) over the entire measurement period were calculated (Table 2). The mean values for N_{AIT} , N_{ACCU} , N_{TOT} , SA_{TOT} , Vol_{TOT} , $D_{\text{p,mode}}$, and BC were $12.4 \times 10^3 \text{ cm}^{-3}$, $18.9 \times 10^3 \text{ cm}^{-3}$, $31.9 \times 10^3 \text{ cm}^{-3}$, $3.4 \times 10^3 \mu\text{m}^2 \text{ cm}^{-3}$, $182 \mu\text{m}^3 \text{ cm}^{-3}$, 117 nm , and $7.96 \mu\text{g m}^{-3}$, respectively. The N_{TOT} was typically within the range observed at other urban locations globally, $(7.6\text{--}32.7) \times 10^3 \text{ cm}^{-3}$ (Table 1). While the N_{TOT} was comparable to that at the urban site, Beijing, in

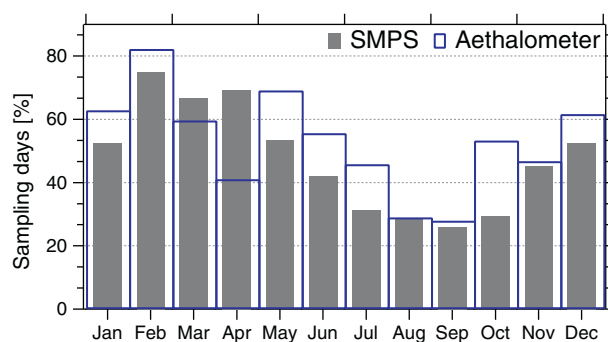


Fig. 2. Sampling days for SMPS and Aethalometer in individual months, summed over the four years of measurements.

China ($32.7 \times 10^3 \text{ cm}^{-3}$) (Wu et al., 2008), it was about 40–80% higher than those reported at other urban areas in developed nations (Table 1). The N_{TOT} was also much higher than that ($21.8 \times 10^3 \text{ cm}^{-3}$) at a semi-urban site, Gual Pahari, in India, mainly attributed to the minimal major local pollution sources (e.g. traffic and residential) at Gual Pahari (Hyvarinen et al., 2010). The mean BC mass concentration was also within the observed range at other urban locations globally, ($0.2\text{--}10.2 \mu\text{g m}^{-3}$) (Ramachandran and Rajesh, 2007 and references therein), and comparable to urban locations such as New Delhi ($0.9\text{--}25.5 \mu\text{g m}^{-3}$) (Tiwari et al., 2013), Ahmedabad, India ($0.2\text{--}10 \mu\text{g m}^{-3}$) and Beijing, China ($8.7\text{--}10.1 \mu\text{g m}^{-3}$), but much higher compared to urban locations in developed countries such as Zurich, Switzerland ($1.7 \mu\text{g m}^{-3}$) and East St. Louis, USA ($0.7\text{--}1.8 \mu\text{g m}^{-3}$) (Ramachandran and Rajesh, 2007).

Fig. 3 illustrates the mean seasonally averaged diurnal variation of N_{AIT} , N_{ACCU} , N_{TOT} , BC, and mixed depth (MD) at Kanpur, over the entire measurement period. At Kanpur, the primary emission of aerosol particles in the Aitken to accumulation mode size range appears to be the main driving force of the diurnal variation in the aerosol concentrations, as opposed to urban location in China (Wu et al., 2008), where frequent NPF events were observed. While the new aerosol production and their subsequent growth can profoundly alter total particle number concentration during the event, the relatively less NPF events observed at Kanpur (Kanawade et al., personal communication), possibly had less/negligible contribution to the total particles. Note that the relative frequency of NPF occurrence at Kanpur is known only for pre-monsoon season. The diurnal variation of particle number and BC mass concentrations followed a very similar trend in all seasons, analogous to previous reports at this site

Table 2

Summary statistics of size-segregated particle number, total surface area, volume, and BC mass concentrations. “±” indicates standard deviation (1σ).

	5%	25%	Median	75%	95%	Mean $\pm \sigma$
$N_{\text{AIT}} [10^3 \text{ cm}^{-3}]$	0.8	3.5	7.7	15.7	39.6	12.4 ± 10.8
$N_{\text{ACCU}} [10^3 \text{ cm}^{-3}]$	1.4	4.5	11.9	25.1	61.6	18.9 ± 16.4
$N_{\text{TOT}} [10^3 \text{ cm}^{-3}]$	2.6	9.3	20.8	42.2	96.9	31.9 ± 29.7
$SA_{\text{TOT}} [10^3 \mu\text{m}^2 \text{ cm}^{-3}]$	0.2	0.8	2.2	4.7	11.4	3.4 ± 3.2
$Vol_{\text{TOT}} [\mu\text{m}^3 \text{ cm}^{-3}]$	9.5	36	114	250	622	182 ± 207
BC [$\mu\text{g m}^{-3}$]	0.2	2.31	5.49	11.3	23.7	7.96 ± 7.78
$D_{p,\text{mode}} [\text{nm}]$	36	85	118	145	201	117 ± 49

based on one-year study (Baxla et al., 2009), with a peak in the morning and late evening hours and minima in the afternoon hours. This could be attributed to the anthropogenic emissions in the local vicinity of the sampling site (traffic, residential and industrial emissions apart from trash/wood burning primarily during winter season). The accumulation mode particles were generally higher than the Aitken mode particles, except in monsoon. This is not surprising considering the fact that the aerosol emissions from residential and/or biomass burning are dominated by accumulation mode particles (Reid et al., 2005), or that the primary emitted small particles further either externally or internally mixed with other aerosol components (Dey et al., 2008; Shamjad et al., 2012). During rainy season, a relatively large fraction of accumulation mode particles can also be effectively removed by wet deposition leading to lower concentrations. A previous study showed that precipitation can effectively scavenge particles either smaller than 30 nm or larger than 400 nm (Laakso et al., 2003). This behavior has also been reported at a variety of locations across the world, including background sites (Hyvärinen et al., 2011; Shen et al., 2011), urban site (Wu et al., 2008) as well as forested environment such as Amazon rainforest (Ahlm et al., 2010). Further, a good correlation between N_{ACCU} and BC concentrations can be seen (Fig. S4). The diurnal variation of particle number and BC mass concentrations was negatively correlated with the planetary boundary layer height, as a result of increased atmospheric dilution (Fig. 3).

Fig. 4 shows the monthly statistics of N_{AIT} , N_{ACCU} , N_{TOT} , SA_{TOT} , Vol_{TOT} , BC, and $D_{p,\text{mode}}$. All parameters, except N_{AIT} , showed a clear monthly variation with the maximum concentration in winter and lower during the monsoon, which is consistent with a previous study at the semi-urban site in India (Hyvarinen et al., 2010). This monthly variation is also consistent with previous investigations in other urban areas globally (Hussein et al., 2004; Puustinen et al., 2007; Stanier et al., 2004; Wehner and Wiedensohler, 2003), but the lower concentration was observed in summer (June–August) at other locations, which is rainy season over India. The lower concentration during the monsoon over the Indian subcontinent can be partly due to efficient wet deposition of aerosol particles by precipitation (Hyvärinen et al., 2011). The highest monthly mean N_{TOT} ($54.2 \times 10^3 \text{ cm}^{-3}$) was observed in January, whereas the lowest ($3.9 \times 10^3 \text{ cm}^{-3}$) was detected in August (Fig. 4c). Similarly, the monthly mean

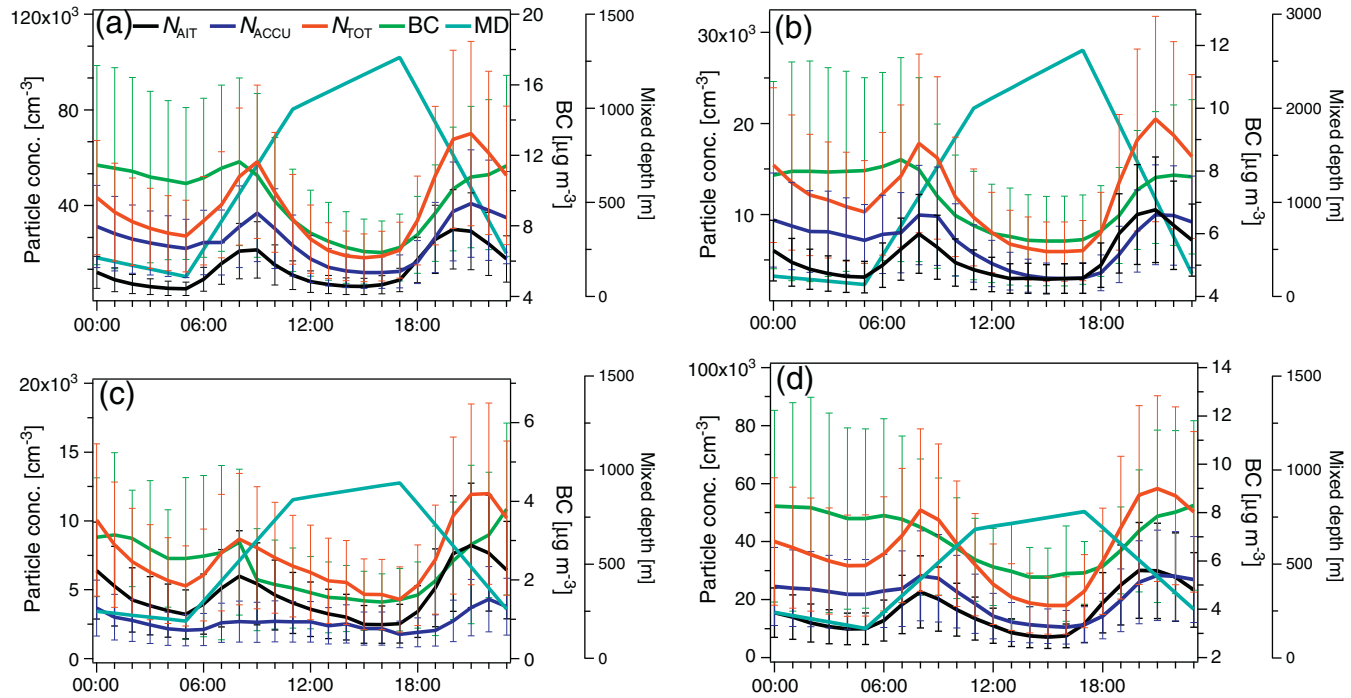


Fig. 3. Mean diurnal variation of size-segregated particle number concentrations, BC and mixed depth (MD) for (a) winter, (b) pre-monsoon, (c) monsoon, and (d) post-monsoon seasons at the Kanpur site. The error bars indicate standard deviation.

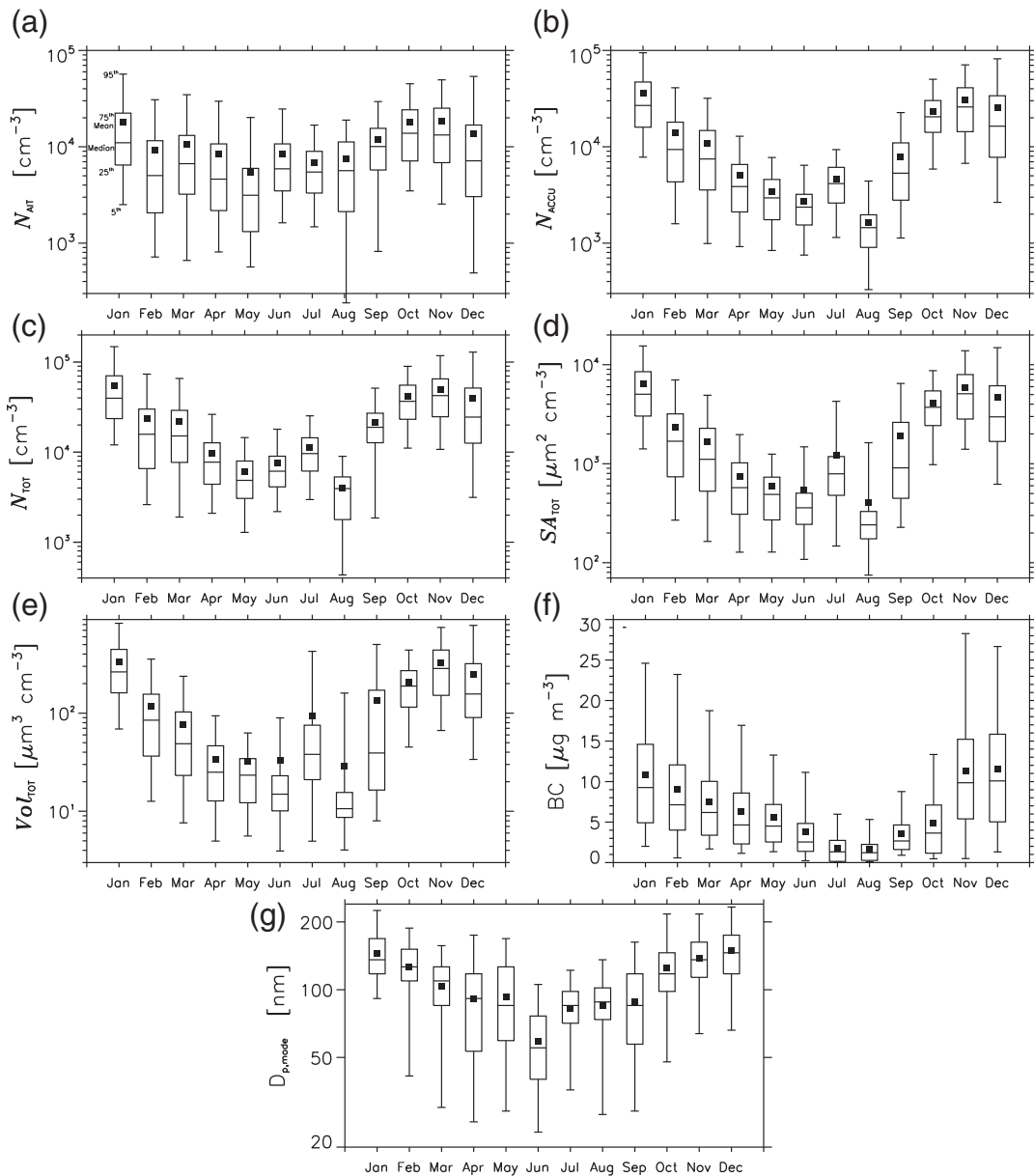


Fig. 4. Statistical analysis of (a) N_{AIT} , (b) N_{ACCU} , (c) N_{TOT} , (d) SA_{TOT} , (e) V_{TOT} , (f) BC concentration, and (g) $D_{p,mode}$. The horizontal solid line indicates the median, filled square indicates the mean, top and bottom of the box indicate the 75th and 25th percentiles, respectively, and top and bottom whiskers indicate the 95th and 5th percentiles, respectively.

BC mass concentration was also the highest ($11.5 \mu\text{g m}^{-3}$) and the lowest ($1.6 \mu\text{g m}^{-3}$) during the winter and monsoon seasons, respectively (Fig. 4f). The seasonal pattern in BC showed a similar pattern to that of N_{TOT} , with a reasonably good correlation coefficient, $R^2 = 0.53$. The $D_{p,mode}$ also showed similar seasonal behavior to that of N_{TOT} (Fig. 4g), with highest during the winter season. Note that there were no long-term ambient measurements for organic carbon (OC). But, a recent study, based on AERONET level-2 data, showed that the OC/BC ratio for Kanpur varies from 1 to 15 (Arola et al., 2011), with high values during post-monsoon and winter (Kaul et al., 2011), indicative of biomass burning

sources, while lower ratios are being associated with fossil-fuel combustion emission (McMeeking et al., 2009). Major sources of energy in India include coal, petroleum, biomass, nuclear power, and hydropower. About 70% of all of India's coal consumption is for power generation that generates almost 60% of total energy required in India (Garg et al., 2002). These power plant facilities are large emitter of carbonaceous aerosols into the atmosphere. There is only one coal-based thermal power plant located about 3 km aerial distance from the IITK site to the southeast that may come in upwind direction occasionally, but this region is also surrounded by a large number of other coal-based facilities.

N_{AIT} showed a less significant seasonal fluctuation. Previous studies in urban areas showed that N_{AIT} was higher than other particle modes, perhaps due to the strong influence of vehicular emissions and frequent occurrence of NPF events (Stanier et al., 2004; Wu et al., 2008). Our recent study at this site during pre-monsoon season (April–May) showed that the latter process does not occur as frequently at other urban locations across the globe, primarily due to large pre-existing particles (Kanawade et al., personal communication). Further, a recent experimental study at this site also showed that the primary emitted BC particles were mostly internally mixed (possibly with different aerosol components) (Shamjad et al., 2012), probably indicative of transported aged particles at the site. These two season-dependent factors might have caused relatively lower seasonal fluctuations in N_{AIT} .

Fig. 5 shows the ratio of Aitken to accumulation mode particles, $N_{\text{AIT}}/N_{\text{ACCU}}$. The Aitken mode dominated the particle number concentration from the middle of pre-monsoon to the early post-monsoon season (Fig. 5), analogous to other semi-urban site in India that is not directly influenced by local traffic and located about 25 km to the south of the major urban center, New Delhi (Hyvarinen et al., 2010; Hyvärinen et al., 2011). Hyvarinen et al. (2010) used this ratio, $N_{\text{AIT}}/N_{\text{ACCU}}$, to determine the age of the air masses. During the pre-monsoon and monsoon seasons, this ratio varied from 0.2 to 7.2 (with a mean value of 1.5) and 0.1 to 14.2 (with a mean value of 3.1), respectively. The high ratio values could arise due to NPF events (Hyvarinen et al., 2010). This is not surprising, considering the fact that newly formed particles (1–20 nm) can effectively grow to Aitken mode sizes (~80 nm) during most NPF events (Kanawade et al., 2012; Kulmala, 2003; Shen et al., 2011), by condensation of various vapors onto the existing particle surface (Kulmala et al., 2001). Higher condensable vapor source rate during the summer (pre-monsoon in this study) was also previously observed based on eight-years of dataset (Dal Maso et al., 2005), leading to faster growth in summer compared to other seasons globally (Kulmala et al., 2004). Further, our recent study at the same site showed that

NPF occurred commonly (~16%) during April–May (Kanawade et al., personal communication). It may be possible that the commonly observed NPF events during the pre-monsoon season lead to higher concentration of Aitken mode particles at this site, apart from other primary sources (e.g. local vehicular emissions etc.). A recent study at a background site, Mukteshwar, in India showed that NPF occurs frequently in pre-monsoon months from March till June (~82%) (Neitola et al., 2011). On the other hand, this ratio varied from 0.1 to 4.8 (with a mean value of 0.6) during the winter. The low value indicates that the air mass was aged and/or contains larger particles as a primary aerosol (Fig. 4f, g). It should be noted that NPF occurs rarely in winter globally (Kulmala et al., 2004; Stanier et al., 2004). Neitola et al. (2011) also reported only sporadic NPF events during post-monsoon and winter season, though from a background site, Mukteshwar, primarily due to lower solar radiation. In developing countries such as India and China, the additional reason could be the pre-existing large particles that may further suppress NPF over these regions, irrespective of the time of the year. Unlike at our site and semi-urban site, Gual Pahari (Hyvarinen et al., 2010) in India, the accumulation mode particle number concentration was always higher at a background site, Mukteshwar (Hyvärinen et al., 2011).

3.3. Seasonal variation of particle number size distributions

In urban areas, the PNSDs may vary rapidly in shape and magnitude due to numerous factors such as primary emissions by mobile (e.g. traffic) and stationary (e.g. power plant) sources (Kim et al., 2002; Morawska, 2002), local meteorology (Wehner and Wiedensohler, 2003), and long-range transport that brings air masses from diverse regions (Birmili et al., 2001). Besides, PNSDs not only vary from year to year, but also vary in individual season of the year. Here, we present seasonally calculated PNSDs over the entire measurement period (Fig. 6). As a measure of variability, the mean, median, 25th and 75th percentiles, and 5th and 95th percentiles were derived for each season. The modal particle number

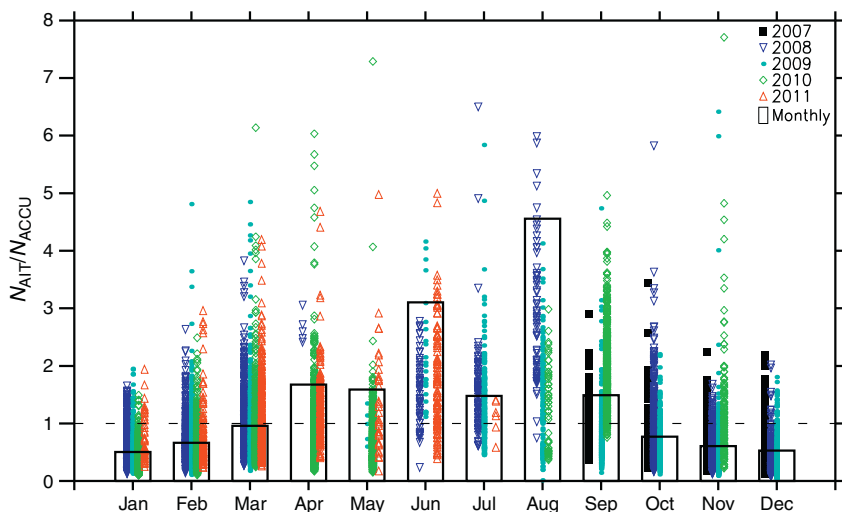


Fig. 5. Monthly variation of the ratio of Aitken to accumulation mode particles, $N_{\text{AIT}}/N_{\text{ACCU}}$. The symbol and vertical bar indicate hourly and monthly averages, respectively.

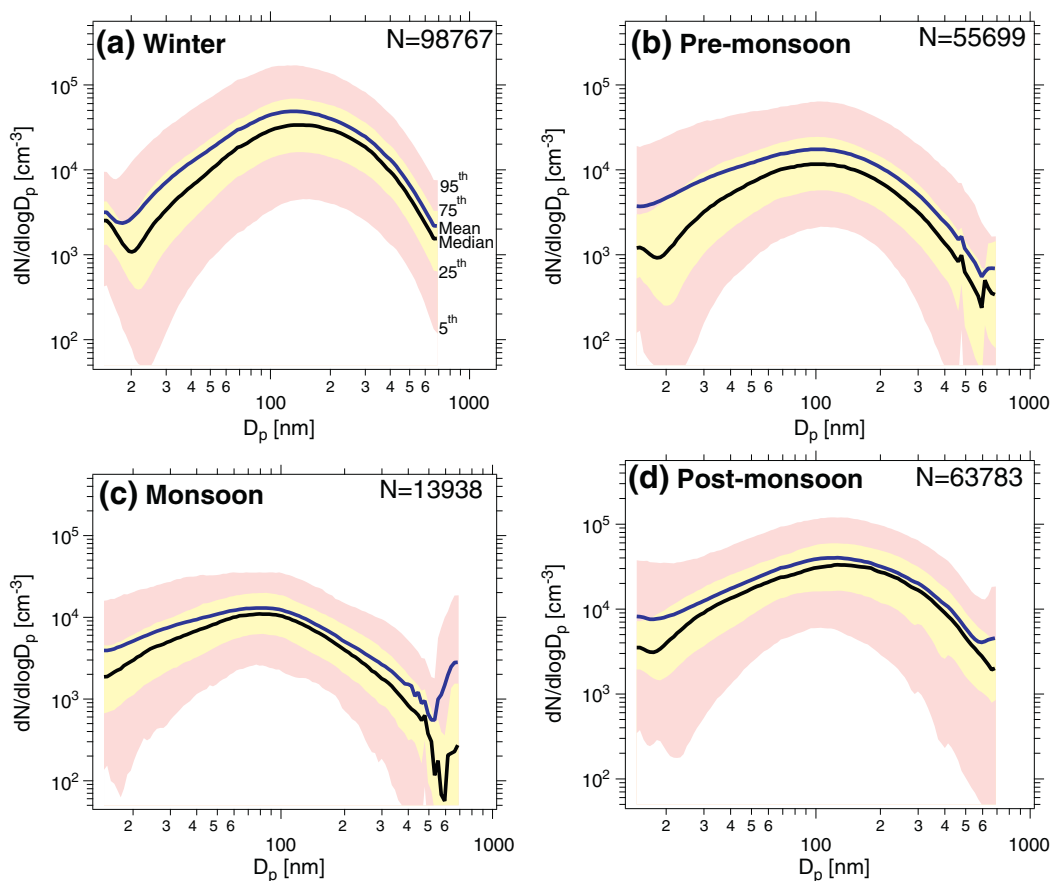


Fig. 6. Seasonally averaged particle number size distributions ($dN/d\log D_p$) based on 5-minute data. N indicates the number of PNSD's averaged for individual season.

concentration (N_g) as well as geometric mean diameter ($D_{p,g}$) show statistically significant differences between individual seasons (Table 3). The lowest particle number concentration was observed in monsoon season, partly due to wet removal of aerosol particles from the atmosphere with the onset of monsoon in late June over this region (Hyvärinen et al., 2011). The width of the distribution (σ_g) was found to be the lowest and highest in winter and post-monsoon seasons, respectively. The differences between individual seasons are also seen in the 5th and 95th percentiles, with the largest interquartile span in winter. Previous study at this site also showed that the difference between the peak values of daytime and nighttime PNSDs was the highest in winter, which was mainly governed by lower temperature and subsequent large

anthropogenic activities (mainly trash/wood burning in addition to cooking, industrial activities and traffic) (Baxla et al., 2009). The characteristics of PNSD between this site and other semi-urban Indian site, Gual Pahari (Hyvärinen et al., 2011) appeared to show distinct behavior. For example, the averaged PNSD during monsoon season at Gual Pahari appeared to be bi-modal with first mode at ~ 20 nm, as opposed to uni-modal at our site. This suggests that comparing PNSDs from a variety of geographical locations require simultaneous long-term measurements, which may eliminate anomalies caused by variations in concurrent meteorological conditions, local emissions, and long-range transport processes.

3.4. Contribution of BrC

In order to determine the major local source (i.e. wood burning vs fossil fuel combustion) of BrC at this site, we have estimated the percentage difference in mass concentrations measured at two different wavelengths i.e. 370 nm and 880 nm, and it is given as $[(BrC_{370nm} - BC_{880nm}) / BC_{880nm}]$. This approach utilizes the enhanced light absorption of wood burning aerosol at near ultraviolet wavelength (370 nm) relative to the light absorption at near-infrared wavelength (880 nm) for fossil fuel combustion aerosols (Herich et al., 2011; Wang et al., 2011b). Fig. 7 shows monthly variation of

Table 3

Statistical parameters [modal number concentration, N_g ; geometric mean diameter, $D_{p,g}$; geometric standard deviation, σ_g] for seasonally averaged particle number size distributions.

	N_g [10^3 cm^{-3}]	$D_{p,g}$ [nm]	σ_g [unitless]
Winter	24.4	134	1.97
Pre-monsoon	8.9	96	2.01
Monsoon	8.5	74	2.06
Post-monsoon	27.6	112	2.16
All	17.1	113	2.07

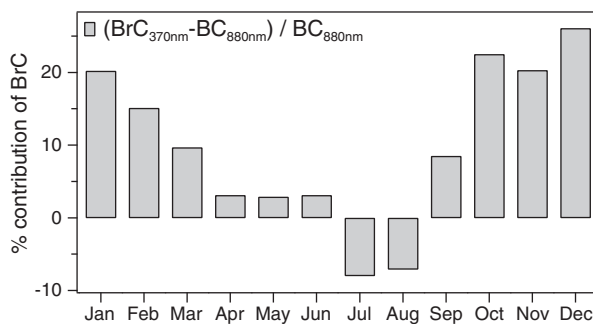


Fig. 7. Monthly variation of the percentage contribution of BrC given by $[(\text{BrC}_{370\text{nm}} - \text{BC}_{880\text{nm}}) / \text{BC}_{880\text{nm}}]$.

$[(\text{BrC}_{370\text{nm}} - \text{BC}_{880\text{nm}}) / \text{BC}_{880\text{nm}}]$ ratio for the Kanpur site. The positive ratio indicated that the significant BrC contribution came from wood/trash burning emissions, which was observed higher during mainly winter months. During pre-monsoon months, this ratio was close to zero or negative, suggested that fossil-fuel combustion largely contributed to BrC compared to the wood burning. A similar trend of the ratio was also observed at other urban location, New Delhi, in India (Srivastava et al., 2012), suggesting that fossil-fuel combustion was the major source of BrC emissions, and biomass burning was mainly dominant during winter months. In India, the relative contributions of fossil-fuel combustion and open biomass burning were estimated to be 25% and 33%, respectively, with bio-fuel combustion (44%) being the largest source of BC emissions (Venkataraman et al., 2005).

4. Conclusions

While numerous studies reported sub-micron PNSDs over the Indian subcontinent, there exists only a few observations over an extended period of time. We presented sub-micron PNSD measurements conducted at an urban location, Kanpur, in India, from September 2007 to July 2011. The diurnal and monthly variations of size-segregated particle number and BC mass concentrations were characterized. The mean particle number concentrations of the Aitken mode (N_{AIT}), accumulation mode (N_{ACCU}), the total particles (N_{TOT}), and BC concentrations were $12.4 \times 10^3 \text{ cm}^{-3}$, $18.9 \times 10^3 \text{ cm}^{-3}$, $31.9 \times 10^3 \text{ cm}^{-3}$, and $7.96 \mu\text{g m}^{-3}$, respectively. While the N_{TOT} at this site was comparable to other urban sites in developing nations such as China, it was about 40–80% higher than those reported at urban sites in developed nations. A similar finding was also observed for BC mass concentrations. Total particle volume concentrations appear to be dominated mainly by the accumulation mode particles, except during the monsoon months due to efficient wet deposition of accumulation mode particles by precipitation. The diurnal variation of the total particle number and BC mass concentrations showed a very similar behavior in all seasons, with the highest variation during morning and late evening hours and the lowest variation during the afternoon hours. This kind of behavior could be attributed to the large primary emissions of aerosol particles (e.g. traffic) and the temporal evolution of planetary boundary layer. The particle number

and BC mass concentrations showed a clear seasonal variation with the maximum in winter and minimum during the monsoon, which is consistent with the previous study at the semi-urban site in India (Hyvarinen et al., 2010). However, Aitken mode particles did not show a clear seasonal fluctuation. The ratio of Aitken and accumulation mode particles, $N_{\text{AIT}}/N_{\text{ACCU}}$, varied from 0.1 to 14.2, with maximum during the monsoon and minimum during the winter, analogous to previous investigations at semi-urban site in India. The high ratio values indicate the growth of newly formed particles and/or primary emitted small particles to Aitken mode sizes; whereas the low values indicate that the air mass was aged and/or contains larger particles as a primary aerosol. The seasonal variation of the PNSDs appeared to be driven by the anthropogenic emissions in the immediate vicinity of this site, with the highest concentrations and interquartile span during winter. The wood/trash burning appeared to be the largest source of BrC emissions in post-monsoon and winter, whereas fossil fuel burning contributed largely in monsoon.

Acknowledgments

SNT acknowledges the funding support from National Academy of Sciences (NAS) (2000002802) and United States Agency for International Development (USAID) (AID-OAA-A-11-00012). The views expressed here are of the authors and do not necessarily reflect of NAS or USAID. We acknowledge NOAA ARL for providing HYSPLIT air mass back trajectory calculations. Authors also acknowledge the Center Pollution Control Board (CPCB, India) for providing PM_{10} data.

Appendix A. Supplementary data

Supplementary data to this article can be found online at <http://dx.doi.org/10.1016/j.atmosres.2014.05.010>.

References

- Ahlm, L., et al., 2010. A comparison of dry and wet season aerosol number fluxes over the Amazon rain forest. *Atmos. Chem. Phys.* 10, 3063–3079.
- Arola, A., et al., 2011. Inferring absorbing organic carbon content from AERONET data. *Atmos. Chem. Phys.* 11, 215–225.
- Asnani, G.C., 1993. *Tropical Meteorology*. Pune, India.
- Baxla, S.P., Roy, A.A., Gupta, T., Tripathi, S.N., Bandyopadhyaya, R., 2009. Analysis of diurnal and seasonal variation of submicron outdoor aerosol mass and size distribution in a northern Indian city and its correlation to black carbon. *Aerosol Air Qual. Res.* 9, 458–469.

- Birmili, W., Wiedensohler, A., Heintzenberg, J., Lehmann, K., 2001. Atmospheric particle number size distribution in central Europe: statistical relations to air mass and meteorology. *J. Geophys. Res.* 32, 5–18.
- Chinnam, N., Dey, S., Tripathi, S.N., Sharma, M., 2006. Dust events in Kanpur, northern India: chemical evidence for source and implications to radiative forcing. *Geophys. Res. Lett.* 33, L08803.
- CPCB, 2012. National ambient air quality status and trends in India-2010. Central Pollution Control Board, Ministry of Environment and Forests (NAAQMS/35/2011–2012).
- Dal Maso, M., et al., 2005. Formation and growth rates of fresh atmospheric aerosols: eight years of aerosol size distribution data from SMEARII, Hyytiälä, Finland. *Boreal Environ. Res.* 10, 323–336.
- Dey, S., Di Girolamo, L., 2011. A decade of change in aerosol properties over the Indian subcontinent. *Geophys. Res. Lett.* 38, L14811.
- Dey, S., Tripathi, S.N., 2008. Aerosol direct radiative effects over Kanpur in the Indo-Gangetic basin, northern India: long-term (2001–2005) observations and implications to regional climate. *J. Geophys. Res.* 113, D04212.
- Dey, S., Tripathi, S.N., Singh, R.P., Holben, B.N., 2004. Influence of dust storms on the aerosol optical properties over the Indo-Gangetic basin. *J. Geophys. Res.* 109, D20211.
- Dey, S., Tripathi, S.N., Mishra, S.K., 2008. Probable mixing state of aerosols in the Indo-Gangetic Basin, northern India. *Geophys. Res. Lett.* 35, L03808.
- Draxler, R.R., Rolph, G.D., 2010. HYSPLIT (HYbrid Single-Particle Lagrangian Integrated Trajectory) Model Access via NOAA ARL READY Website. NOAA Air Resources Laboratory, Silver Spring, MD, (<http://ready.arl.noaa.gov/HYSPLIT.php>).
- Eck, T.F., et al., 2010. Climatological aspects of the optical properties of fine/coarse mode aerosol mixtures. *J. Geophys. Res.* 115, D19205.
- Garg, A., Kapshe, M., Shukla, P.R., Ghosh, D., 2002. Large point source (LPS) emissions from India: regional and sectoral analysis. *Atmos. Environ.* 36, 213–224.
- Herich, H., Hueglin, C., Buchmann, B., 2011. A 2.5 year's source apportionment study of black carbon from wood burning and fossil fuel combustion at urban and rural sites in Switzerland. *Atmos. Atmos. Meas. Tech.* 4, 1409–1420.
- Hussein, T., et al., 2004. Urban aerosol number size distributions. *Atmos. Chem. Phys.* 4, 391–411.
- Hyvärinen, A.-P., et al., 2010. Aerosol measurements at the Gual Pahari EUCAARI station: preliminary results from in-situ measurements. *Atmos. Chem. Phys.* 10, 7241–7252.
- Hyvärinen, A.-P., et al., 2011. Effect of the summer monsoon on aerosols at two measurement stations in Northern India – part 2: physical and optical properties. *Atmos. Chem. Phys.* 11, 8283–8294.
- Jai Devi, J., et al., 2011. Observation-based 3-D view of aerosol radiative properties over Indian Continental Tropical Convergence Zone: implications to regional climate. *Tellus B* 63, 971–989.
- Joshi, M., et al., 2012. Harmonisation of nanoparticle concentration measurements using GRIMM and TSI scanning mobility particle sizers. *J. Nanoparticle Res.* 14, 1–14.
- Kanamitsu, M., 1989. Description of the NMC global data assimilation and forecast system. *Weather Forecast.* 4, 335–342.
- Kanawade, V.P., Tripathi, S.N., 2006. Evidence for the role of ion-induced particle formation during an atmospheric nucleation event observed in Tropospheric Ozone Production about the Spring Equinox (TOPSE). *J. Geophys. Res.* 111, D02209.
- Kanawade, V.P., Benson, D.R., Lee, S.-H., 2012. Statistical analysis of 4-year observations of aerosol sizes in a semi-rural continental environment. *Atmos. Environ.* 59, 30–38.
- Kanawade V.P., et al., 2014. Personal communication.
- Kaskaoutis, D.G., et al., 2012. Variability and trends of aerosol properties over Kanpur, northern India using AERONET data (2001–10). *Environ. Res. Lett.* 7, 024003.
- Kaskaoutis, D.G., et al., 2013. Aerosol properties and radiative forcing over Kanpur during severe aerosol loading conditions. *Atmos. Environ.* 79, 7–19.
- Kaul, D.S., Gupta, T., Tripathi, S.N., Tare, V., Collett Jr., J.L., 2011. Secondary organic aerosol: a comparison between foggy and nonfoggy days. *Environ. Sci. Technol.* 45, 7307–7313.
- Kim, S., Shen, S., Sioutas, C., Zhu, Y., Hinds, W., 2002. Size distributions and diurnal and seasonal trends of ultrafine particles in source and receptor sites of the Los Angeles basin. *J. Air Waste Manage. Assoc.* 52, 297–307.
- Komppula, M., et al., 2009. Physical properties of aerosol particles at a Himalayan background site in India. *J. Geophys. Res.* 114, D12202.
- Kulmala, M., 2003. How particles nucleate and grow. *Science* 302, 1000–1001.
- Kulmala, M., et al., 2001. On the formation, growth, and composition of nucleation mode particles. *Tellus* 53B, 479–490.
- Kulmala, M., et al., 2004. Formation and growth rates of ultrafine atmospheric particles: a review of observations. *J. Aerosol Sci.* 35, 143–176.
- Laakso, L., et al., 2003. Ultrafine particle scavenging coefficients calculated from 6 years field measurements. *Atmos. Environ.* 37, 3605–3613.
- Makela, J.M., et al., 1997. Observations of ultrafine aerosol particle formation and growth in boreal forest. *Geophys. Res. Lett.* 24, 1219–1222.
- Matsui, H., et al., 2013. Spatial and temporal variations of new particle formation in East Asia using an NPF-explicit WRF-chem model: north-south contrast in new particle formation frequency. *J. Geophys. Res.* 118 (11,647–611,663).
- McMeeking, G.R., et al., 2009. Emissions of trace gases and aerosols during the open combustion of biomass in the laboratory. *J. Geophys. Res.* 114, D19210.
- McMurry, P.H., et al., 2005. A criterion for new particle formation in the sulfur-rich Atlanta atmosphere. *J. Geophys. Res.* 110, D22502.
- Mejia, J.F., Wraith, D., Mengersen, K., Morawska, L., 2007. Trends in size classified particle number concentration in subtropical Brisbane, Australia, based on a 5 year study. *Atmos. Environ.* 41, 1064–1079.
- Mönkkönen, P., et al., 2005. Measurements in a highly polluted Asian mega city: observations of aerosol number size distribution, modal parameters and nucleation events. *Atmos. Chem. Phys.* 5, 57–66.
- Moorthy, K.K., Suresh Babu, S., Manoj, M.R., Satheesh, S.K., 2013. Buildup of aerosols over the Indian Region. *Geophys. Res. Lett.* 40, 1011–1014.
- Morawska, L., Jayarantne, E.R., Mengersen, K., Thomas, S., 2002. Differences in airborne particle and gaseous concentrations in urban air between weekdays and weekends. *Atmos. Environ.* 36, 4375–4383.
- Neitola, K., et al., 2011. New particle formation infrequently observed in Himalayan foothills – why? *Atmos. Chem. Phys.* 8447–8458.
- Padma Kumari, B., Londhe, A.L., Daniel, S., Jadhav, D.B., 2007. Observational evidence of solar dimming: offsetting surface warming over India. *Geophys. Res. Lett.* 34, L21810.
- Pierce, J.R., Adams, P.J., 2009. Uncertainty in global CCN concentrations from uncertain aerosol emission and primary emission rates. *Atmos. Chem. Phys.* 9, 1339–1356.
- Puustinen, A., et al., 2007. Spatial variation of particle number and mass over four European cities. *Atmos. Environ.* 41, 6622–6636.
- Ram, K., Sarin, M.M., Tripathi, S.N., 2010. Inter-comparison of thermal and optical methods for determination of atmospheric black carbon and attenuation coefficient from an urban location in northern India. *Atmos. Res.* 97, 335–342.
- Ramachandran, S., Rajesh, T.A., 2007. Black carbon aerosol mass concentrations over Ahmedabad, an urban location in western India: comparison with urban sites in Asia, Europe, Canada, and the United States. *J. Geophys. Res.* 112, D06211.
- Ramachandran, S., Ghosh, S., Verma, A., Panigrahi, P.K., 2013. Multiscale periodicities in aerosol optical depth over India. *Environ. Res. Lett.* 8, 014034.
- Ramanathan, V., Ramana, M.V., 2005. Persistent, widespread, and strongly absorbing haze over the Himalayan Foothills and the Indo-Gangetic Plains. *Pure Appl. Geophys.* 162, 1609–1626.
- Ramanathan, V.M., et al., 2008. Atmospheric Brown Clouds: Regional Assessment Report with Focus on Asia. UNEP, Nairobi.
- Reche, C., et al., 2011. New considerations for PM, Black Carbon and particle number concentration for air quality monitoring across different European cities. *Atmos. Chem. Phys.* 11, 6207–6227.
- Reid, J.S., Koppmann, R., Eck, T.F., Eleuterio, D.P., 2005. A review of biomass burning emissions part II: intensive physical properties of biomass burning particles. *Atmos. Chem. Phys.* 5, 799–825.
- Rodríguez, S., et al., 2007. A study on the relationship between mass concentrations, chemistry and number size distribution of urban fine aerosols in Milan, Barcelona and London. *Atmos. Chem. Phys.* 7, 2217–2232.
- Roy, A.A., Baxla, S.P., Gupta, T., Bandyopadhyaya, R., Tripathi, S.N., 2009. Particles emitted from indoor combustion sources: size distribution measurement and chemical analysis. *Inhal. Toxicol.* 21, 837–848.
- Salma, I., et al., 2011. Production, growth and properties of ultrafine atmospheric aerosol particles in an urban environment. *Atmos. Chem. Phys.* 11, 1339–1353.
- Shamjad, P.M., et al., 2012. Comparison of experimental and modeled absorption enhancement by black carbon (BC) core polydisperse aerosols under hygroscopic conditions. *Environ. Sci. Technol.* 46, 8082–8089.
- Shen, X.J., et al., 2011. First long-term study of particle number size distributions and new particle formation events of regional aerosol in the North China Plain. *Atmos. Chem. Phys.* 11, 1565–1580.
- Shi, J.P., Harrison, R.M., 1999. Investigation of ultrafine particle formation during diesel exhaust dilution. *Environ. Sci. Technol.* 33, 3730–3736.
- Singh, A., Dey, S., 2012. Influence of aerosol composition on visibility in megacity Delhi. *Atmos. Environ.* 62, 367–373.
- Singh, R.P., Dey, S., Tripathi, S.N., Tare, V., Holben, B., 2004. Variability of aerosol parameters over Kanpur, northern India. *J. Geophys. Res.* 109, D23206.

- Srivastava, A.K., Singh, S., Pant, P., Dumka, U.C., 2012. Characteristics of black carbon over Delhi and Manora Peak – a comparative study. *Atmos. Sci. Lett.* 13, 223–230.
- Srivastava, M., et al., 2013. CCN closure results from Indian Continental Tropical Convergence Zone (CTCZ) aircraft experiment. *Atmos. Res.* 132–133, 322–331.
- Stanier, C.O., Khlystov, A.Y., Pandis, S.N., 2004. Ambient aerosol size distributions and number concentrations measured during the Pittsburgh Air Quality Study (PAQS). *Atmos. Environ.* 38, 3275–3284.
- Tiwari, S., et al., 2013. Diurnal and seasonal variations of black carbon and PM_{2.5} over New Delhi, India: influence of meteorology. *Atmos. Res.* 125–126, 50–62.
- Tripathi, S.N., Dey, S., Tare, V., Satheesh, S.K., 2005. Aerosol black carbon radiative forcing at an industrial city in northern India. *Geophys. Res. Lett.* 32, L08802.
- Tripathi, S.N., et al., 2006. Measurements of atmospheric parameters during Indian Space Research Organization Geosphere Biosphere Programme Land Campaign II at a typical location in the Ganga basin: 1. Physical and optical properties. *J. Geophys. Res.* 111, D23209.
- Venkataraman, C., Habib, G., Eiguren-Fernandez, A., Miguel, A.H., Friedlander, S.K., 2005. Residential biofuels in South Asia: carbonaceous aerosol emissions and climate impacts. *Science* 307, 1454–1456.
- Wang, K., Dickinson, R.E., Liang, S., 2009. Clear sky visibility has decreased over land globally from 1973 to 2007. *Science* 323, 1468–1470.
- Wang, Y., Hopke, P.K., Chalupa, D.C., Utell, M.J., 2011a. Long-term study of urban ultrafine particles and other pollutants. *Atmos. Environ.* 45, 7672–7680.
- Wang, Y., Hopke, P.K., Rattigan, O.V., Zhu, Y., 2011b. Characterization of ambient black carbon and wood burning particles in two urban areas. *J. Environ. Monit.* 13, 1919–1926.
- Weber, R.J., et al., 1997. Measurements of new particle formation and ultrafine particle growth rates at a clean continental site. *J. Geophys. Res.* 102, 4375–4385.
- Wehner, B., Wiedensohler, A., 2003. Long term measurements of submicrometer urban aerosols: statistical analysis for correlations with meteorological conditions and trace gases. *Atmos. Chem. Phys.* 3, 867–879.
- Weingartner, E., et al., 2003. Absorption of light by soot particles: determination of the absorption coefficient by means of aethalometers. *J. Aerosol Sci.* 34, 1445–1463.
- Woo, K.S., Chen, D.R., H., P.D.Y., McMurry, P.H., 2001. Measurement of Atlanta aerosol size distributions: observation of ultrafine particle events. *Aerosol Sci. Technol.* 34, 75–87.
- Wu, Z., et al., 2008. Particle number size distribution in the urban atmosphere of Beijing, China. *Atmos. Environ.* 42, 7967–7980.
- Young, L.-H., et al., 2013. New particle growth and shrinkage observed in subtropical environments. *Atmos. Chem. Phys.* 13, 547–564.
- Zhang, R., 2010. Getting to the critical nucleus of aerosol formation. *Science* 328, 1366–1367.